Superlattices and Microstructures 47 (2010) 219–224

Contents lists available at ScienceDirect

Superlattices and Microstructures

journal homepage: www.elsevier.com/locate/superlattices

Bragg reflector by means of the form birefringence effect in dielectric rings

Alessandro Massaro *, Roberto Cingolani, Massimo De Vittorio, Adriana Passaseo [1]

National Nanotechnology Laboratory of CNR-INFM, Distretto Tecnologico-ISUFI, Università del Salento, Via Arnesano, 73100 Lecce, Italy

ARTICLE INFO

Article history:
Available online 6 June 2009

Keywords:
Bragg reflector
Form birefringence
Optical dielectric rings

ABSTRACT

In this work, form birefringence physics and the mechanisms of Si/SiO_2 dielectric concentric optical rings are investigated. The optical rings are modeled by means of a Bragg reflector. Similarly to a negative uniaxial crystal, the dielectric concentric pattern admits two preferred propagation directions defined by an extraordinary and an ordinary refractive index representing two field polarizations. The circular grating profile splits the electromagnetic field into a radial (extraordinary field) and a tangential (ordinary field) component which represent two modes of the periodic structure. These two modes are characterized by the refractive index ellipse obtained by the Huygens principle. The model is developed through the wave front propagation inside the anisotropic structure. The Bragg theory and conservation of momentum vectors provide the Bragg angles of the ordinary and extraordinary rays for different optical wavelengths. The Bragg theoretical model is validated by the finite difference time domain (FDTD) approach for a wavelength of $\lambda = 0.98\ \mu m$.

1. Introduction

The birefringent properties of crystals may be explained in terms of the anisotropic electrical properties of the molecules of which the crystals are composed. Birefringence may, however, arise from anisotropy on a scale much larger then molecular, namely when there is an order arrangement

* Corresponding author. Tel.: +39 0832 298373; fax: +39 0832 298386.
E-mail address: alessandro.massaro@unile.it (A. Massaro).
[1] Permanent address: IMM-CNR sezione Lecce, University Campus, Lecce-Monteroni 73100, Italy.

0749-6036/$ – see front matter © 2009 Elsevier Ltd. All rights reserved.
doi:10.1016/j.spmi.2009.05.003

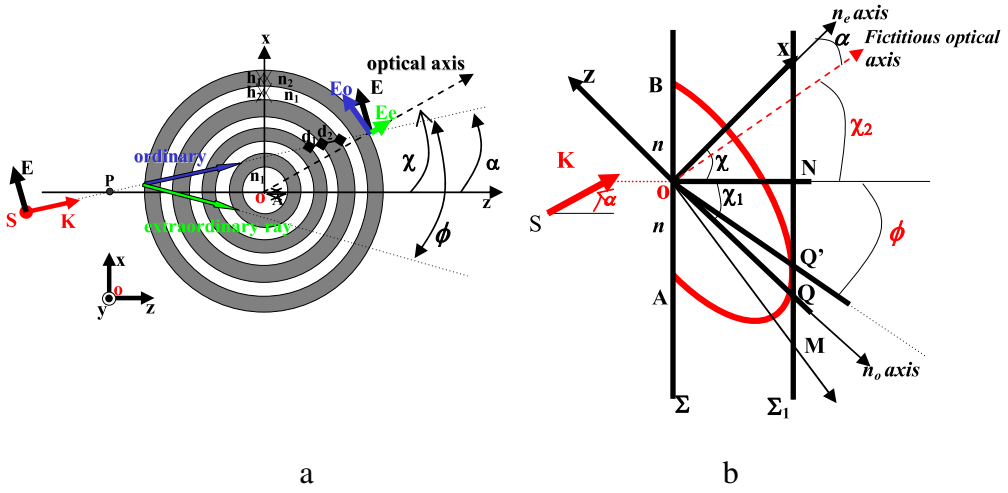

Fig. 1. (a) Birefringence form in optical dielectric rings. (b) Wave front and refractive index ellipse related to the dielectric rings at a particular propagation time.

of similar particles of optically isotropic material whose size is large compared with the dimensions of molecules, but small compared with the wavelength of light. We then speak of form birefringence. The form birefringence performs the important function of separating an incident beam into two orthogonally polarized outgoing parallel beams. Such function can be accomplished by isotropic periodic dielectric structures that can split an incident beam into two preferred directions as in a uniaxial crystal, Bragg reflectors, and polarization splitters [1–15]. Previous works have analyzed the form birefringence effect generated in thin dielectric parallel plates [2,5] or in an oblique deposited film composed of dielectric microcolumns and voids [4]. In this work we study the same anisotropic effect generated in dielectric rings: the circular pattern is well suited for applications where degenerate modes, correlated to the polarization [10,11], are confined in a central microcavity with different wavelengths. As in Bragg reflectors, by applying the Bragg theory to the dielectric rings, we consider these degenerate modes as Bragg reflected modes. The presence of degenerate modes such as ordinary and extraordinary modes is explained by the form birefringence effect. From optical theory [2,5], the form birefringence is analyzed by considering the idealized case of a regular assembly of particles that have the form of thin parallel plates. In this case two types of thin dielectric film, with low and high refractive indices, alternate periodically, and the thicknesses of the layers are sufficiently small compared with the working optical wavelength λ_0. With respect to the ring configuration of Fig. 1(a), the same birefringence effect is obtained for particular incidence angles α of the wave source represented by a vector **K** [11]. The wave vector **K**, with incidence angle α, generates in the circular pattern an ordinary $\mathbf{E}_o$ component (characterized by the ordinary n_o refractive index) and an extraordinary $\mathbf{E}_e$ one (characterized by the extraordinary n_e refractive index) which are tangential and radial to the rings, respectively (see Fig. 1(a)). The ordinary and the extraordinary refractive indices are evaluated by the refractive index ellipse of Fig. 1(b) defined by the wave front at a particular propagation time and incidence angle α [11]: the n_e axis is defined along the x-direction and coincides with the optical axis which is orthogonal to the dielectric rings of Fig. 1(a) and defined by the incidence angle α, while the n_o axis is defined along the z-direction. The $n = n_e(\chi)$ value changes with the direction of **K** and characterizes the split angle ϕ of the two modes for a particular incidence angle α.

In this work we analyze the form birefringence in Si/SiO_2 dielectric rings through the wave front propagation (described by the Huygens principle) and the Bragg diffraction theory. The Bragg theory and the conservation of momentum vectors provide the Bragg angles of the ordinary and extraordinary rays for different optical wavelengths. The Bragg angles, which display maximum intensity as a result of constructive interference, are verified through two-dimensional (2D) finite

difference time domain (FDTD) modeling. We summarize the presented work in the following points: (i) we analyze the form birefringence of the Si/SiO_2 dielectric rings through the form birefringence theory by providing the analytical expressions of the refractive indices; (ii) we analyze the Bragg condition and the conservation momentum vector of the Si/SiO_2 dielectric ring for different ring thicknesses and different working wavelengths; (iii) finally we validate the theoretical by means of a 2D FDTD numerical simulation.

2. Form birefringence and wave propagation in dielectric optical rings

The split angle ϕ reported in Fig. 1(a) and (b) defines the directions of the ordinary and extraordinary modes of the proposed Bragg reflector. The relationship between the split angle ϕ and the incidence angle α is estimated by means of the Huygens principle, starting from the ordinary and extraordinary wave fronts [2,3,5]: the ordinary and the extraordinary wave fronts can be superimposed to the indices' ellipse for particular τ values (τ is the propagation time of the wave front in the periodic structure). As reported in Fig. 1(b), Σ_1 is the envelope, at time $t+\tau$, of wavelets emitted from the various points of the wave front Σ at time t. We see that ON/τ is the velocity of the wave and OQ/τ is the propagation velocity of the ray. By considering the reference system of Fig. 1(a) and a wavelet centered at O, the refractive index ellipse is defined by $\chi_1 = \pi/2 - \chi$, $d\chi = -d\chi_1$, $x = -n\cdot\cos\chi, z = -n\cdot\sin\chi$, where $n = n_e(\chi) = OB = OA$ is the refractive index of the Σ envelope. The ellipse equation in the x–z-plane of Fig. 2(b) for an optical axis orientation χ is

$$\frac{\cos^2\chi}{n_e^2} + \frac{\sin^2\chi}{n_o^2} = \frac{1}{n^2}. \tag{1}$$

We observe that the fictitious axis of Fig. 1(b) characterizes the refractive index ellipse for a generic incidence angle α.

By differentiation, we get [3,5]

$$\frac{dn}{d\chi} = n^3\cdot\left(\frac{1}{n_e^2} - \frac{1}{n_o^2}\right)\cdot\sin\chi\cdot\cos\chi \tag{2}$$

where the relation between the angle ϕ (the split angle between the ordinary and the extraordinary optical ray) and the variation of the refractive index n with respect to the angle χ is as follows [3,5]:

$$\tan\phi = -\frac{1}{n}\cdot\frac{dn}{d\chi} = -n^2\cdot\left(\frac{1}{n_e^2} - \frac{1}{n_o^2}\right)\cdot\sin\chi\cdot\cos\chi \tag{3}$$

with

$$n^2 = \frac{n_e^2\cdot n_o^2}{n_o^2\cdot\sin^2\chi_1 + n_e^2\cdot\cos^2\chi_1} \tag{4}$$

and

$$\begin{aligned} n_e^2 &= \frac{n_1^2 n_2^2}{f_1 n_2^2 + f_2\varepsilon_1}, \\ n_o^2 &= f_1 n_1^2 + f_2 n_2^2 \end{aligned} \tag{5}$$

where $f_1 = 1-f_2$, and f_2 represent the dielectric filling factors [2,11]. For a particular value of incidence angle α and positions P (see Fig. 1(a)), the filling factors f_1 and f_2 of the ring structure are obtained by [2, 11]

$$\begin{aligned} f_1 &= \frac{\sum_n d_{n1}}{\sum_n d_{n1} + \sum_m d_{m2}}, \\ f_2 &= \frac{\sum_n d_{n2}}{\sum_n d_{n1} + \sum_m d_{m2}} \end{aligned} \tag{6}$$

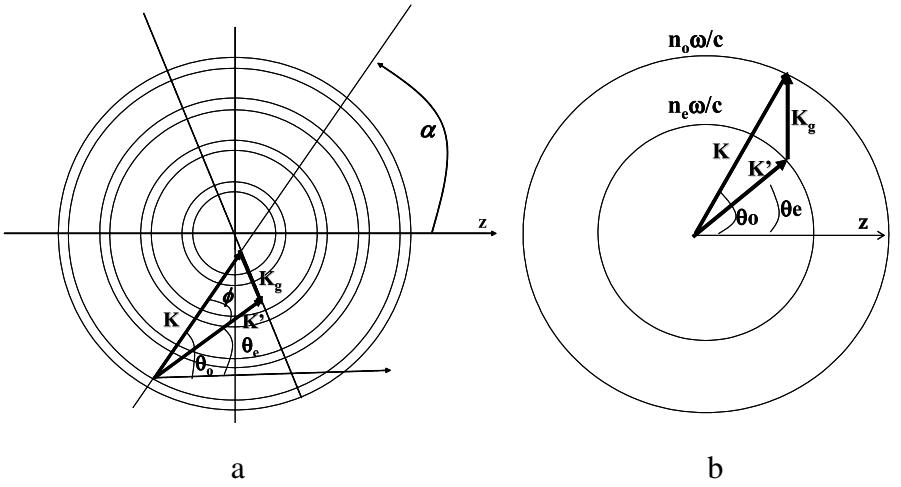

Fig. 2. Anisotropic Bragg scattering and momentum vectors in the ring structure.

where d_{n1} and d_{m2} (see Fig. 1(a)) are the segments defined through the intersection between the line corresponding to the wave vector (line of equation $x = (z + \mathrm{OP}) \tan\alpha$) and the circles of the rings.

We observe that for a particular incidence angles (ordinary Bragg angles) $\alpha = \theta_o$ the split angle ϕ is equal to $\theta_o - \theta_e$, where θ_e is the extraordinary Bragg angle obtained by the Bragg scattering theory.

3. Bragg theory and results

The concentric rings generates, as in a birefringent device, an ordinary and an extraordinary optical ray. For a particular incidence angle α in the z–x-plane, the ordinary and the extraordinary rays are characterized by momentum conservation, which defines the Bragg diffraction condition. This condition provides the maximum intensity of these two generated modes (ordinary and extraordinary modes) as a result of constructive interference. The relationships between the ordinary θ_o and the extraordinary θ_e Bragg angles reported in Fig. 2(a) are obtained by the following considerations. The circular structure presents different gratings with the angle α varying in the plane, so the light diffraction by gratings can be pictured as an interaction process between the incident wave and the diffracted wave [7–9]. In a birefringent medium, the refractive index associated with a light beam is dependent on the propagation direction. The diffracted light beam propagates in a different direction from the incident beam and so we can associate the ordinary index n_o with the incident beam (wave vector $|\mathbf{K}| = n_o\omega/c$) and the extraordinary index n_e with the diffracted beam (wave vector $|\mathbf{K}'| = n_e(\chi)\omega/c$). Momentum conservation requires that the incident wave vector, the diffracted wave vector and the grating wave vector of the ring structure $\mathbf{K}_g$ $(2\pi/h)$ form a triangle, where h is the sum $h_1 + h_2$. Let θ_o and θ_e be the angles between the light beams and the $\mathbf{K}_g$-wave vector of the grating. The Bragg diffraction conditions are obtained from the triangle of Fig. 2(b), and are given by [5,7,8]

$$2h \sin\theta_o = \frac{\lambda_0}{n_o} - \frac{h^2}{n_o\lambda_0}(n_e^2(\chi_1) - n_o^2) \tag{7}$$

$$2h \sin\theta_e = \frac{\lambda_0}{n_e(\chi_1)} - \frac{h^2}{n_e(\chi_1)\lambda_0}(n_e^2(\chi_1) - n_o^2). \tag{8}$$

According to Eqs. (7) and (8), the angles of both light beams are function of (λ_0/h) when n_o and $n_e(\chi_1)$ are fixed. Bragg diffraction is only possible when [5,7,8]

$$|n_o - n_e(\chi_1)| \le \lambda_o/h \le |n_o + n_e(\chi_1)| \tag{9}$$

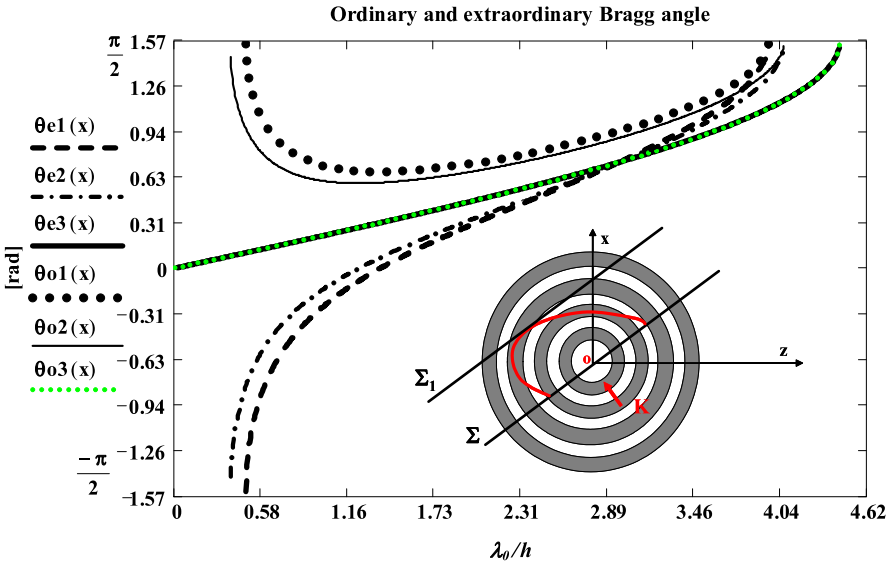

Fig. 3. Ordinary (θ_o) and extraordinary (θ_e) angles as function of the ratio between the working wavelength λ_0 and the radial period $h = h_1 + h_2$ in the case of concentric SiO_2 rings ($n_1 = 1.465$) and Si rings ($n_2 = 3.24$) for $\alpha = \pi/3$ rad, $\chi = 1.25$ rad, OP $= 39.29\ \mu$m (θ_{e1} and θ_{o1} plots), for $\alpha = \pi/6$ rad, $\chi = 0.93$ rad, OP $= 38.5\ \mu$m (θ_{e2} and θ_{o2} plots), and for $\chi = 0$, OP $= 0$ (θ_{e3} and θ_{o3} plots). The ring structure is characterized by $h_1 = 0.2\ \mu$m, $h_2 = 0.1\ \mu$m and $A = 40\ \mu$m. Inset: superposition of the refractive index ellipse defined in Fig. 1(b) with the Bragg reflector of Fig. 1(a).

Table 1
Calculated ϕ_c and numerical ϕ_n split angles. The numerical values are obtained by the 2D FDTD approach. The ring structure is characterized by $h_1 = 0.2\ \mu$m, $A = 40\ \mu$m, $\alpha = \pi/3$ rad, $\chi = 1.25$ rad, and $\lambda_0 = 0.98\ \mu$m.

h_2 (μm)	OP (μm)	n_o	n_e	$n_e(\chi)$	ϕ_c (deg.)	ϕ_n (deg.)
0.1	39.29	2.220	1.708	1.744	0.170	0.156
0.15	39.92	2.392	1.804	1.844	0.297	0.260
0.2	40.12	2.514	1.887	1.929	0.403	0.375
0.25	40.31	2.605	1.961	2.005	0.495	0.462
0.3	40.54	2.675	2.026	2.070	0.573	0.551
0.35	40.8	2.731	2.084	2.129	0.647	0.620

and the angles θ_o and θ_e are real. We observe that, for a source S placed at O, the extraordinary refractive ellipse degenerates in a circumference with radius n_o and $\theta_o = \theta_e$ ($\mathbf{K}'$ and $\mathbf{K}$ are collinear) according to conservation of momentum reported in Fig. 2(b). In Fig. 3 we show the calculated Bragg angles of the proposed $Si(n_2 = 3.24)/SiO_2(n_1 = 1.465)$ Bragg reflector of Fig. 1(a) versus the working wavelengths and versus the parameter $h = h_1 + h_2$. The Bragg angles of Eqs. (7) and (8) are obtained for different χ angles defined by the source position and by the incidence angle α. The ordinary and the extraordinary refractive indices of Eqs. (7) and (8) are calculated by Eqs. (3), (5) and (6) through the refractive index ellipse construction of Fig. 1(b) (reported also in the inset of Fig. 3).

We validate the Bragg angle calculation through a 2D FDTD approach. Fig. 4 shows the calculated and the simulated split angles $\phi = \theta_o - \theta_e$ versus h_2 by considering $\lambda_0 = 0.98\ \mu$m, $h_1 = 0.2\ \mu$m and $A = 40\ \mu$m: according to Fig. 3 the split angle ϕ increases with the parameter h_2. Moreover, Fig. 4 shows the ordinary and the extraordinary ray intensities and the FDTD modeling. The FDTD split angles are obtained by considering the geometrical construction reported in the inset of Fig. 4, which considers the distance L of the ordinary and the extraordinary intensity (L is distance between the intensity peaks) shown in a reference plane placed at the output of the Bragg reflector. A low error of 0.02 rad between the simulation and the calculation is observed, thereby confirming the accuracy of the analytical model. Table 1 shows all parameters obtained during the calculation of the split angles of Fig. 4.

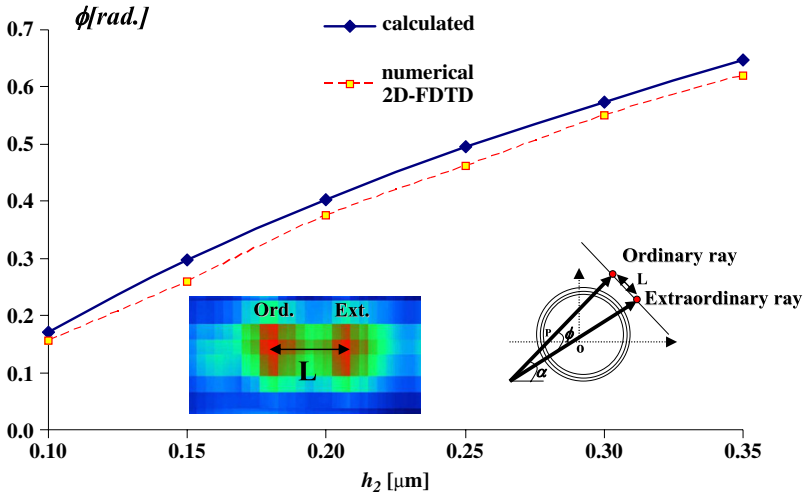

Fig. 4. Calculated and simulated (FDTD approach) split angles $\phi = \theta_o - \theta_e$ versus h_2, by considering the Bragg condition. The ring structure is characterized by $h_1 = 0.2\ \mu m$, $A = 40\ \mu m$, $\alpha = \pi/3$ rad, $\chi = 1.25$ rad, and $\lambda_0 = 0.98\ \mu m$. Inset: ordinary and extraordinary rays and 2D FDTD modeling.

4. Conclusion

In this work we have presented a theoretical model by which the birefringent effects of concentric dielectric rings at optical frequencies can be analyzed. Particular Bragg incidence angles select two main modes, indicated as ordinary and extraordinary modes, which propagate in the proposed Si/SiO_2 Bragg reflector. The Bragg angles and the split angles of the two modes for different wavelengths and incidence angles have been computed with the developed model. The theoretical computations have been validated with numerical results obtained using the finite time domain (FDTD) method. This model can also be applied to circular photonic crystals with microcavities.

References

[1] F. Abelès, Ann. Phys. 5 (1950) 596.
[2] M. Born, E. Wolf, Principles of Optics, 6th ed., U.K. Cambridge Univ. Press, Cambridge, 1980.
[3] B. Rossi, Optics, Addison-Wesley, 1967.
[4] K. Shiraishi, K. Matsumura, IEEE J. Quantum Electron. 30 (1994) 2417.
[5] A. Massaro, L. Pierantoni, T. Rozzi, IEEE J. Quantum Electron. 40 (2004) 821.
[6] A.D. Remenyuk, E.V. Astrova, T.S. Perova, V.A. Tolmachev, J. Vij, A. Moore, ICTON Conference Proceeding 1 (2003) 269.
[7] P. Pochi Yeh, Introduction to Photorefractive Nonlinear Optics, Wiley-Interscience, New York, 1993.
[8] P. Yeh, Optical Waves in Layered Media, Wiley, New York, 1988.
[9] A. Yariv, Optical Waves in Crystals, Wiley, New York, 1984.
[10] A. Tandaechanurat, S. Iwamoto, M. Nomura, N. Kumagai, Y. Arakawa, Opt. Express 16 (2008) 448.
[11] A. Massaro, V. Errico, R. Cingolani, M. De Vittorio, A. Passaseo, IEEE J. Quantum Electron. 44 (2008) 1225.
[12] P.T. Lee, T.W. Lu, F.M. Tsai, IEEE Photonics Technol. Lett. 19 (2007) 710.
[13] P.T. Lee, T.W. Lu, J.H. Fan, F.M. Tsai, Appl. Phys. Lett. 90 (2007) 151125.
[14] J. Scheuer, A. Yariv, IEEE J. Quantum Electron. 39 (2003) 1555.
[15] J. Scheuer, A. Yariv, Phys. Rev. E 70 (2004) 036603.